Microscopic calculation of dielectric tensor of quaterthiophene crystals

M. Laicini,[1,*] P. Spearman,[2] S. Tavazzi,[1] and A. Borghesi[1]
[1]*INFM and Dipartimento di Scienza dei Materiali, Università Milano-Bicocca, Via Cozzi 53, I-20125 Milano, Italy*
[2]*School of Chemical and Pharmaceutical Sciences, Penrhyn Road, Kingston upon Thames, Surrey KT1 2EE, United Kingdom*
(Received 14 May 2004; revised manuscript received 24 September 2004; published 26 January 2005)

We present a microscopic calculation of the dielectric tensor for a quaterthiophene crystal near resonances of Frenkel excitons in a vibronic coupling regime. We show how the intermolecular interactions modify the intensity and energy of each vibronic level from the isolated molecule to the solid state after transverse excitation. In particular, a strong redistribution of oscillator strength is found between the vibronic levels of the upper Davydov state. On the basis of the calculated dielectric tensor, we reproduce the measured absorbance spectra as recorded in different experimental configurations taking into consideration the additional role of the longitudinal macroscopic field. Some replicas in the optical spectra are clearly attributable to transitions of Frenkel origin while the role of other types of excitons, such as those of charge-transfer parentage is also discussed.

DOI: 10.1103/PhysRevB.71.045212 PACS number(s): 71.35.Cc, 78.20.Ci, 78.40.Me

I. INTRODUCTION

Over recent years there has been an increasing interest in using molecular materials in optical and electrical devices in order to take advantage of their vast range of properties and design capability. Most notably, they are used either in polymer form benefiting from their easy processibility, or as thin films of vacuum evaporated short chain oligomers. In both cases there is a relatively high degree of disorder between the molecular units. Although there are only weak van der Waals forces binding the molecules in the solid, their excited-state properties are highly dependent on their mutual distribution. In crystals, excitonic co-operative excited states can be generated that may determine the bulk absorptive and emissive properties rather than be dominated by the individual molecular spectral characteristics.[1]

Most theoretical investigations that are related to the photophysics of conjugated organic polymers have been carried out on isolated chains—approximating behavior in dilute solutions or matrix host materials. Nevertheless, conjugated polymers can be viewed as a collection of interacting finite-size segments and display similar properties to molecular crystals, and concepts developed for these materials are being widely applied to longer chain conjugated polymers. Molecular exciton theory is very versatile and is able to cope with macroscopic systems and adapt to the level of interactions between neighboring chromophores. In the past, theoretical approaches were applied to relatively small molecules that can form crystals, but more recently, research and development interest has focused on conjugated chain oligomers that have lengths greatly exceeding the intermolecular distance, which possess strong optical transitions in the visible region. For example, it has been demonstrated as a basis for understanding the excited state dynamics in polycrystalline materials, or aggregates.[2,3] In the weak interaction limit, spectroscopic properties can be obtained via a first-order perturbation treatment, whereas in the strong interaction limit, the excitation is delocalized over several molecules, and a more appropriate description of crystal eigenstates requires the building of delocalized wave functions.[4,5] However, this has a cost in computability and to date, only clusters of molecules have been treated. To overcome such a limitation, the molecular exciton theory has been adapted using a more sophisticated atomic charge transition density exciton model to represent the delocalized molecular transition dipole.[6] This has the advantage that calculations can cover much larger networks, and models can be applied to emulate real films and bulk crystals.

As a model material, oligothiophene *nT* has been extensively studied and despite the high technological interest, the fundamental optical properties of oligothiophene crystals, as well as thin films, remain somewhat ambiguous.[7] Interpretation of their optical properties has relied on various theoretical approaches[8–13] with different approximations, and faced with a wide variety of experimental data[14–22] that are affected by film morphologies or crystal quality. These crystals are generally leaflike and exhibit only one crystallographic developed plane, which poses a limitation on the experimental interpretation of the optical spectra, though it may be significant in determining operation of such materials in devices because of the natural confinement of the emission within the crystal plane boundaries.

Such systems crystallize in a monoclinic structure (see Fig. 1)[23] and exhibit strong anisotropic optical properties originating from two different types of excitation: Frenkel excitons (FEs) and charge transfer excitons (CTEs). As for FE states the lowest excited molecular state is transformed in the crystal into one strong transition polarized in the *ac* plane and another weak transition at lower energy polarized along the *b* crystal axis, the Davydov splitting (DS) between them being a measure of the intermolecular interaction. These transitions can be excited at normal incidence on the usual accessible face. For *ac* polarization, a strong peak is indeed observed, together with shoulders on the low-energy side. These shoulders have been discussed in terms of either FE or CTE states. Similarly, the weaker component shows some sharp well-defined peaks in low-temperature spectra that have been discussed in terms of phonon modes as well as a series of broad replica whose parentage as either FE or CTE has not been unequivocally determined.[12,15,20] Given this

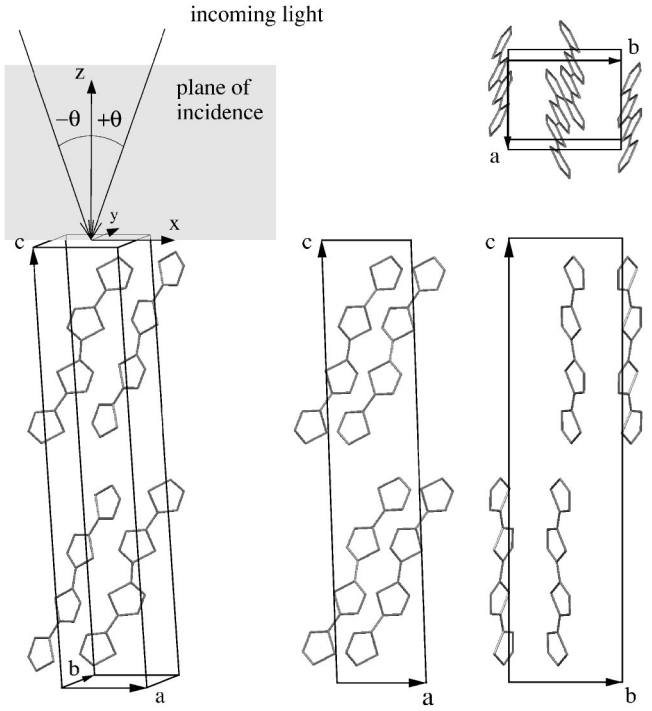

FIG. 1. The monoclinic unit cell of 4-*T* crystal as taken from Ref. 23. The projections show the orientation of the molecule with respect to the crystal axes a,b,c. The x,y,z system is also sketched with x and y parallel to a and b axis, respectively, while the z axis is normal to the ab face. The angle of incidence θ is shown together with the conventional sign adopted in this work. The crystallographic data are the following: $a=6.085$ Å, $b=7.858$ Å, $c=30.483$ Å, and $\beta=91.81°$.

background, we present a fully microscopic calculation of the dielectric tensor of a 4-*T* bulk crystal near resonances of mechanical Frenkel excitons. We start from single effective vibronic excitations of the isolated molecule and calculate the actual excitonic eigenstates resulting from electrostatic interactions between excited molecules described by atomic charge densities and find a redistribution of predominant excitations in energy and intensity for both polarizations. The model ignores light coupling since it is a small correction.[24] From this calculation we are able to simulate the experimental configurations demonstrated by angle dependent measurements of polarized spectra and such a comparison allows us to discriminate between FE and CTE states.

II. MODEL

The crystal Frenkel excitons originating from the first molecular excited state are described in Heitler-London approximation by the Hamiltonian[4,25]

$$H=\sum_{\mathbf{n}} H_{\mathbf{n}}+\frac{1}{2}\sum_{\mathbf{n}\neq\mathbf{m}} V_{\mathbf{n},\mathbf{m}}, \tag{1}$$

where $H_{\mathbf{n}}$ is the Hamiltonian of a "free" molecule on site $\mathbf{n}$ and $V_{\mathbf{nm}}$ the electrostatic interaction between site $\mathbf{n}$ and $\mathbf{m}$ responsible for the delocalization of excitation throughout the crystal. The eigenfuctions of $H_{\mathbf{n}}$ are chosen to be Born-Oppenheimer separable with an effective vibrational mode that summarize the response of all other coupled modes and they form a basis from which to determine the crystal exciton eigenstates.[26]

Once the crystal states are built from Bloch plane waves the Frenkel exciton Hamiltonian can be block diagonalized by means of a unitary transformation that acts on the electronic part of wave functions.[2,27] This diagonalization leads to distinctive polarized exciton wave functions (Davydov states) that form bases for the irreducible representations of the factor group of the crystal.[11,22,28] In the case of a monoclinic unit cell with four molecules, Eq. (1) evaluated at the center of Brillouin zone reduces to

$$H_{\mathrm{exc}}=\begin{bmatrix} H_{a_g} & & & \\ & H_{a_u} & & \\ & & H_{b_g} & \\ & & & H_{b_u} \end{bmatrix}. \tag{2}$$

Each vibrational block, with α symmetry ($\alpha\equiv\{a_g a_u b_g b_u\}$) includes interactions between different vibronic excitons of the same polarization and reads

$$H_{\alpha}=\sum_{\nu} E_{0\nu}|\nu\rangle\langle\nu|+\sum_{\nu\mu} T_{\alpha} S_0^{\nu} S_0^{\mu}|\nu\rangle\langle\mu|. \tag{3}$$

In this equation, $\{|\nu\rangle\}$ are vibrational functions describing the nuclear motions in the electronic excited state; $E_{0\nu}=E_{00}+D+\nu\hbar\omega$ where E_{00} is the energy difference between the two minima of the molecular vibronic transition, D is the gas-to-crystal shift energy and $\nu\hbar\omega$ is the vibrational energy of ν quanta of the effective mode. In the second term of Eq. (3), $S_0^{\nu}(S_0^{\mu})$ is the Franck-Condon overlap factor for the transition from the zero vibrational mode of the ground electronic state to $\nu(\mu)$ vibrational mode of excited state both described in harmonic approximation. T_{α} refers to the resonance energy of the α Davydov state whose value is obtained by linear combinations of the pair electronic interactions I between the excited molecules in the crystal:

$$\begin{aligned} T_{a_g} &= I_{AA}+I_{AB}+I_{AC}+I_{AD},\\ T_{a_u} &= I_{AA}+I_{AB}-I_{AC}-I_{AD},\\ T_{b_g} &= I_{AA}-I_{AB}+I_{AC}-I_{AD},\\ T_{b_u} &= I_{AA}-I_{AB}-I_{AC}+I_{AD}, \end{aligned} \tag{4}$$

where A,B,C,D refer to the four molecules in the unit cell. The transfer energies I have to be calculated for a crystal array of Coulombic interacting dipoles that represent the molecular electronic transition in the first excited state. In oligothiophene crystals the distance between neighboring molecules is less than a third of the length of the molecule. Thus we prefer to describe the molecular delocalized dipole as a distribution of point charges located on atomic sites. The values are calculated from an *ab initio* atomic orbital decomposition of the HOMO-LUMO first electronic transition.[26,29] In order to take into account the long-range nature of Cou-

TABLE I. Resonance energies (eV) and transition dipole moments (Debye) as obtained from numerical diagonalization of a_u and b_u vibronic sub-blocks in Eq. (3) with the following parameters: effective vibrational mode energy $\hbar\omega=1470\ \mathrm{cm}^{-1}$ (Refs. 9, 32, and 33), Huang-Rhys factor $\lambda^2=1.35$ (Ref. 33), $E_{00}+D=2.70$ eV; calculated values for the transfer energies: $T_{a_u}=-0.114$ eV and $T_{b_u}=0.275$ eV. The latter are obtained using the following parameters: molecular dipole moment $|\mathbf{d}|=11.9$ D (Refs. 21 and 34); static dielectric tensor $\varepsilon_{xx}=3.08, \varepsilon_{yy}=2.42, \varepsilon_{zz}=5.49$ (Refs. 35–40).

	a_u		b_u	
ν	Ω_ν	d_ν	Ω_ν	d_ν
0	2.65	0.726	2.74	6.012
1	2.84	0.587	2.95	8.780
2	3.04	0.407	3.15	11.925
3	3.23	0.269	3.31	13.998
4	3.42	0.163	3.45	9.620
5	3.60	0.089	3.62	4.224
6	3.78	0.044	3.78	1.704

lomb interactions the summation of interactions between the two molecular distributions of charges is performed via Ewald method for a three-dimensional system with inclusion of screening by a static dielectric constant according to $r_i'=r_i/\sqrt{\epsilon_{ii}^0}$.[30,31] The Ewald method separates the actual interaction into two contributions: a transverse inner field and a longitudinal macroscopic term. As the resonances of the dielectric tensor occur at the transverse energies of the excitons, we consider only the inner field part of the Coulombic interaction.[25]

The numerical diagonalization of the vibronic sub-block of well defined symmetry α in Eq. (3) leads to the resonances and transition dipole moments for each vibronic exciton state. From these values, reported in Table I, the dielectric tensor is subsequently built as follows:

$$\varepsilon_{ij}(\omega)=\varepsilon_\infty\delta_{ij}+\frac{1}{\varepsilon_0 V\hbar}\sum_\alpha\sum_\nu\frac{d^i_{\alpha\nu}d^j_{\alpha\nu}\Omega_{\alpha\nu}}{\Omega^2_{\alpha\nu}-\omega^2-i\gamma(\omega)\omega}. \quad (5)$$

ε_∞ is the isotropic high-frequency dielectric constant, $d^i_{\alpha\nu}$ is the i component of the resulting exciton dipole moment of ν replica with α symmetry, the resonances $\Omega_{\alpha\nu}$ are eigenvalues of the vibronically coupled system, and $\gamma(\omega)$ is the damping factor chosen to be linear with frequency [$\gamma(\omega)=0.03\ \omega$].

By numerical diagonalization of Eq. (5), we find one of the principal axes of the dielectric tensor parallel to the monoclinic axis, the other two lying in the *ac* plane. These latter axes are also subject to axial dispersion, i.e., they rotate in the plane with frequency even if negligible in the region of the first strong transition. With respect to these principal axes, the tensor in Eq. (5) is given by

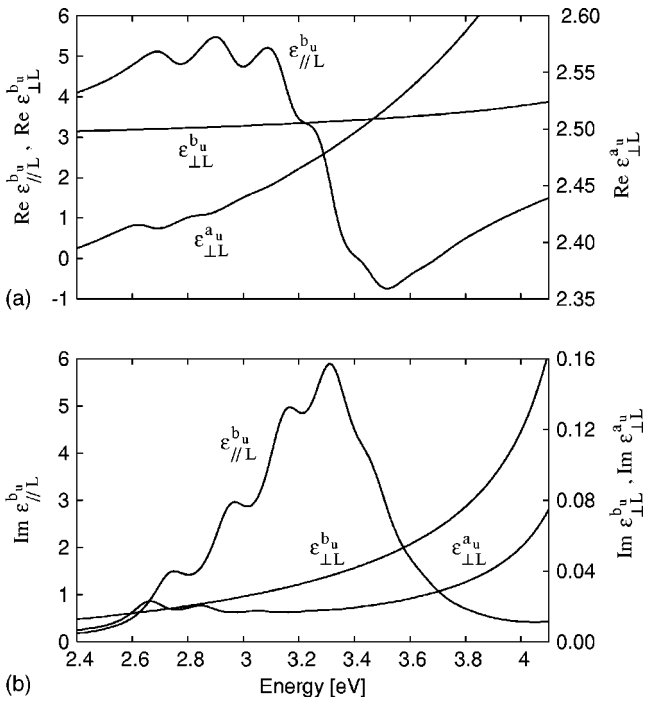

FIG. 2. Calculated real (a) and imaginary (b) parts of the components of the dielectric tensor in its diagonal form [Eq. (6)] with $\varepsilon_\infty=2.1$.

$$\varepsilon(\omega)=\begin{bmatrix}\varepsilon^{b_u}_{\perp L(ac)} & & \\ & \varepsilon^{a_u}_{\perp L(b)} & \\ & & \varepsilon^{b_u}_{\parallel L(ac)}\end{bmatrix}, \quad (6)$$

the eigenvalue $\varepsilon^{a_u}_{\perp L(b)}$ referring to the a_u transition, $\varepsilon^{b_u}_{\parallel L(ac)}$ and $\varepsilon^{b_u}_{\perp L(ac)}$ to the b_u. Figure 2 reports both real and imaginary part of the three resulting components of Eq. (6). Furthermore, Fig. 3 shows how the electronic interaction among molecules is responsible for the line shape of the imaginary part. Indeed for the noninteracting system (i.e., when the electronic interaction among molecules is zero), $\varepsilon^{b_u}_{\parallel L(ac)}$ and $\varepsilon^{a_u}_{\perp L(b)}$ have exactly the same shape: the latter is only less intense, simply as a result of the geometric projection of the transition dipole onto the *b* axis. The eigenstates and eigenvalues of such an unrealistic system are equivalent to an oriented gas model (OGM) whose crystal eigenstates are simply built from a superposition of isolated molecular ones.

Switching on the electronic interaction leads to a coupling among the zero-order vibronic eigenstates of the crystal due to the nonvanishing off-diagonal terms of each vibronic sub-block. These interactions are responsible for a modification of the energy levels and a revising of the corresponding oscillator strengths. The solid lines sketched on the floor in Fig. 3 represent the vibronic energy levels as a function of electronic interaction between molecules, while their slopes are proportional to the oscillator strength of the corresponding level.[41] The way this perturbation acts depends on the sign of electrostatic energy interaction T_α. For the lower a_u Davydov

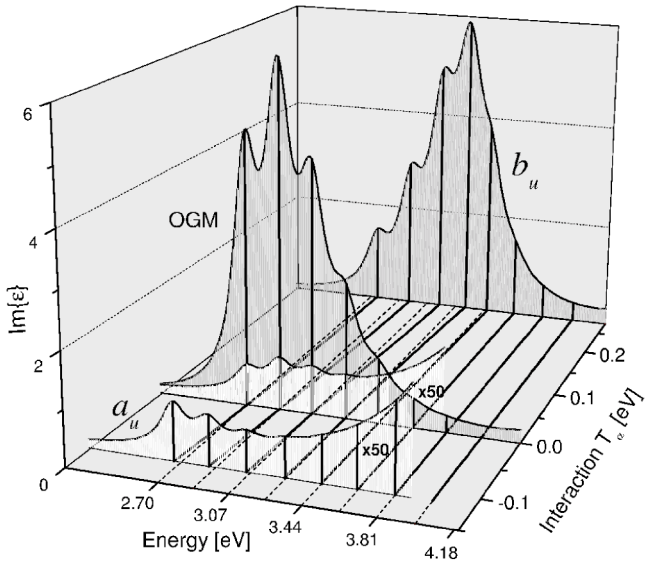

FIG. 3. Imaginary part of the dielectric tensor components $\varepsilon^{b_u}_{\|L(ac)}, \varepsilon^{a_u}_{\perp L(b)}$ for different electronic interaction energies T_α. In particular, the curve labeled OGM represents the noninteracting case with $T_\alpha=0$. The continuous lines on the floor refer to the energy positions of exciton states as a function of resonance interaction. The dashed lines indicate the unperturbed energies of the starting molecular vibronic levels.

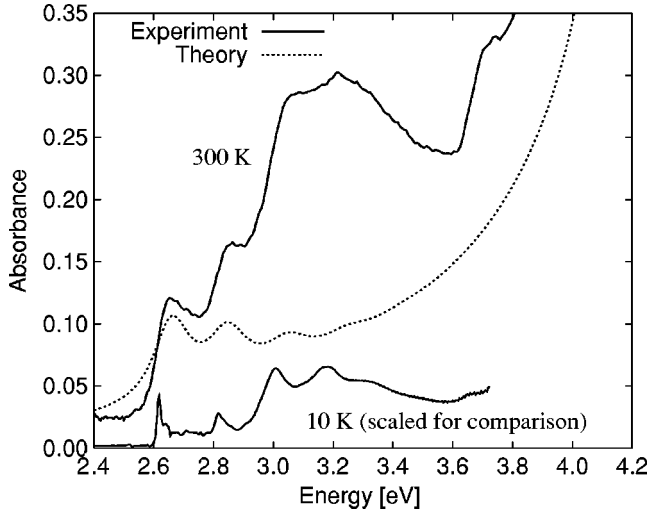

FIG. 4. *b*-polarized absorbance spectra of 4-*T* crystals at normal incidence on the *ab* face as measured at room and low temperatures (continuous lines) and calculated spectrum (dashed line).

component the stabilization energy moves the levels towards the low part of the spectrum and accommodates the lower replica. On the contrary, a positive perturbation representing the upper b_u Davydov state results in a blueshift and a favoring of higher replica. The actual eigenstates and eigenvalues are no longer the same as the isolated molecules. They possess an effective Franck-Condon factor lesser or greater than the starting molecular one. Moreover, the energy spacing between different vibronic states is no longer regular as in the oriented gas model.

Even if the oligothiophene accessible face prevents the most intense transverse component of the b_u transition to be detected, results on 5-*T* nanocrystals show good agreement with this microscopic calculation. In particular the optical functions reported in Ref. 16 reveal the same vibronic structure and similar irregular energy spacing between the shoulders. Moreover, the dielectric functions reported in the literature[19,42] show the main resonance at about the same energy as in Fig. 2 even if pure electronic transitions are usually considered thus representing an envelope of the vibronic transitions shown here.

III. EXPERIMENTAL AND CALCULATED SPECTRA

Absorbance spectra (defined as $-\log_{10}$ of transmittance) of 4-*T* single crystals of the low-temperature polymorph[23] were taken with *p* and *s* polarization and *ac* as plane of incidence, with an apparatus described elsewhere[19] and the thickness of the sample was measured with a Nanoscope IIIa atomic force microscope equipped with a *J*-type scanner.

The two excited waves inside the system are solutions of the Fresnel dispersion relations: one is a completely transverse propagating wave (ordinary wave), while the other (extraordinary wave) also contains a longitudinal field component due to a macroscopic polarization of the medium and gives rise to the well-known directional dispersion.[43] This term can be computed from Ewald's method, which depends on the angle between the propagating wave vector inside the crystal and the exciton transition dipole moment. Another way of studying the macroscopic field effect, once the transverse dielectric tensor is known, is to look for the zero of the loss function $k_i\varepsilon_{ij}(\omega)k_j$. Unfortunately, as discussed in Ref. 44, the availability of only a single surface prevents exploring the entire stopping band with optical measurements. In order to simulate the different absorbance spectra from the calculated dielectric tensor we built up the 4×4 transfer matrix for an arbitrarily anisotropic slab.[45,46] This formalism connects the complex amplitudes of the *p* and *s* modes of incident and reflected waves with the two transmitted amplitudes, and in addition accounts for all multiple reflections inside the sample.

A. Ordinary wave: *b*-polarized spectra

Figure 4 shows the *b* polarized spectrum as measured at normal incidence and at different temperatures on few-μm-thick crystals of 4 *T*. In the room temperature spectrum there are two well defined peaks centered at 2.65 and 2.84 eV, and a broad band with recognizable structures at 3.04 and 3.21 eV which are better resolved in the low-temperature spectrum; there are also shoulders above 3.60 eV followed by a very steep tail due to higher excited states that are expected to have a strong intensity in the *b* polarization as they originate from excitations parallel to molecular short axis *M*. With a dashed line we show the calculated spectrum for a slab of the same thickness. This figure clearly shows that we are able to reproduce the positions of the first two peaks, especially in the room-temperature spectrum, since we only consider a single effective vibrational mode that summarizes

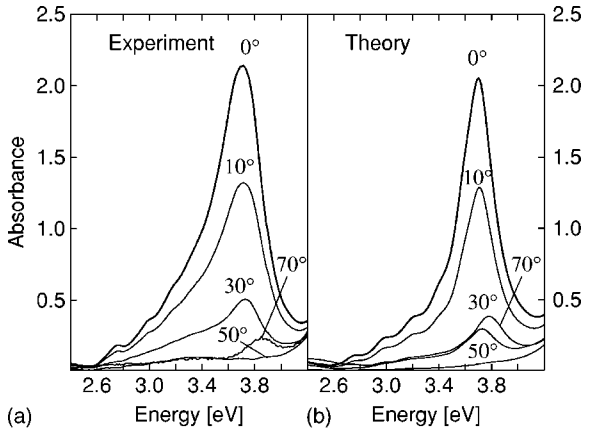

FIG. 5. Experimental spectra of a 280±50-nm-thick crystal (a) and calculated spectra for a 300-nm-thick crystal (b) at different angles of incidence on the 4-*T ab* face, *p* polarization, and *ac* as plane of incidence.

the room-temperature response of all the other vibrational modes. Thus within this approximation the peak at 2.64 eV is attributed to the 00 replica of the lower Davydov state. The second one separated by 0.19 eV is the 01 replica whose intensity we expect to be less than the purely electronic 00 transition as also seen in low-temperature measured absorption. At higher energy only the theoretical spectra reproduce the third and fourth vibronic structures, which are concealed by the broad band between about 3.0 and 3.5 eV in the experimental spectrum. The origin of this structure should be of CTE parentage similar to that reported for 6-*T* crystals in the literature, where the low coupling between CTE and FE is also discussed.[13] Hence our simulated spectra based only on FE states are unable to reproduce the intensities and correct positions of those upper structures.

B. Extraordinary wave: *ac*-polarized spectra

With incident light on the *ab* face and *ac* polarization, a mixed transverse and longitudinal wave propagates. Due to the relatively steep orientation of the molecule to the accessible crystal face, the longitudinal fraction is quite considerable being proportional to $(\mathbf{k}\cdot\mathbf{d})^2$, $\mathbf{k}$ being the propagating wave vector. As discussed elsewhere[15,42,44] this electrodynamic effect causes not only a modification of energy positions but it is responsible also for a further revision of the corresponding oscillator strengths with respect to those values characterizing the dielectric tensor. Thus for the system under investigation the absorbance line shape is expected to be quite different from the imaginary part the the dielectric tensor.

In order to investigate the extraordinary response we performed the absorbance measurements on the crystal by varying the angle of incidence as sketched in Fig. 1. The results are reported in Fig. 5(a). The spectra at normal incidence and low angles are characterized by the main peak at 3.7 eV, a series of shoulders 2.75, 2.97, 3.20 eV, and a weak structure at 3.40 eV. As discussed in Refs. 42 and 44 even by varying the direction of the incident light, the detected resonances do not shift appreciably. The only visible effect is a progressive reduction of the intensity. This is due to the limited range of angles that can be probed inside the crystal with vacuum as incident medium. As the incident angle is varied in the positive direction the propagating wave vector approaches the direction of the exciton transition dipole with a consequent reduction in the projection of the exciting electric field. At +50° the absorption disappears corresponding to a refracted extraordinary wave vector real and parallel to the transition dipole moment.

Within 4×4 formalism and with the calculated dielectric tensor we simulate the spectra for the same experimental configurations and the results are reported in Fig. 5(b). The overall line shape and the position of the typical 4-*T* absorption structures are well reproduced. To obtain the best matching between experimental and simulated intensity, a thickness of 300 nm has been adopted. This value is in very good agreement with the experimental one for the measured crystal (280±50 nm), thus further confirming the validity of the calculated dielectric tensor. Taking a closer look at the normal incident spectra one notes differences between simulated and experimental spectra evident in the energy region where CTE can play an important contribution (about 3.0–3.5 eV). By the arguments given above it is possible to attribute the origin of each peak to vibronic replica of FEs. Moreover, if we look for energy separations between them, we find values greater than the starting effective mode energy corresponding to those calculated and shown in Fig. 3. For higher replica no structures can be recognized and they collapse into a single main peak centered at 3.7 eV.

IV. CONCLUSIONS

Based on Frenkel excitons we have presented a microscopic calculation of dielectric tensor for a prototypical system such as a quaterthiophene crystal by calculating the actual crystal eigenvalues and eigenstates necessary to describe the photophysics of this important class of materials. In particular these new eigenstates of the exciton Hamiltonian describe the real collective response of molecules over which the excitation is delocalized due to a nonzero electronic interaction between them. This resonance energy removes the degeneracy of the oriented gas model levels leading to a DS for each molecular vibronic state. Moreover, we have found a redistribution of oscillator strengths among replica as well as a modification of their energy spacing before being further divided by the electrodynamic (macroscopic polarization) mechanism. Thus the DS depends on Frank-Condon factors of each resonance. Another view of looking at DS can be the difference between the two maxima of the polarizations. In the transverse configuration it is given as 0.66 eV, while the experimental measurement at normal incidence, which naturally contains the macroscopic part is about 1 eV, which is frequently quoted in the literature.

Moreover, from a quantitative direct comparison between measured and calculated spectra in different experimental configurations, we have gained more insight into the origin of some structures observed in room-temperature absorbance spectra. In particular within this model we identify the first

two peaks of the *b* polarized spectrum as the first and second replica of the lower Davydov state originating from a Frenkel exciton. Since electron exchange is not included in our calculation the region above 3 eV which displays evidence of CTEs is not fully treated. On the contrary, for the other polarization the resulting oscillator strengths of vibronic replica are much greater and thus dominate the shape of the spectra even if they can be affected by CTEs between 3.0 and 3.5 eV.

ACKNOWLEDGMENTS

We wish to thank Reinhard Scholz, Marco Bernasconi, and Piotr Petelenz for useful discussions.

*Electronic address: Marco.Laicini@mater.unimib.it

[1] M. Pope and C. E. Swenberg, *Electronic Processes in Organic Crystals and Polymers*, II edition (Oxford University Press, Oxford, 1999).
[2] I. Vragovic and R. Scholz, Phys. Rev. B **68**, 155202 (2003).
[3] S. Blumstengel, F. Meinardi, P. Spearman, A. Borghesi, R. Tubino, and G. Chirico, J. Chem. Phys. **117**, 4517 (2002).
[4] A. S. Davydov, *Theory of Exciton* (Plenum Press, New York, 1971).
[5] M. R. Philpott, Annu. Rev. Phys. Chem. **31**, 97 (1980).
[6] S. Marguet, D. Markovitsi, P. Millié, H. Sigal, and S. Kumar, J. Phys. Chem. B **102**, 4697 (1998).
[7] D. Fichou, *Handbook of Oligo- and Poly-Thiophenes* (Wiley-VCH, Weinheim, 1999).
[8] D. Beljonne, J. Cornill, R. Silbey, P. Millié, and J. L. Bredas, J. Chem. Phys. **112**, 4749 (2000).
[9] H. Sun, Z. Zhao, F. C. Spano, D. Beljonne, J. Cornil, Z. Shuai, and J. L. Bredas, Adv. Mater. (Weinheim, Ger.) **15**, 818 (2003).
[10] F. C. Spano, J. Chem. Phys. **118**, 981 (2003).
[11] M. Muccini, M. Schneider, C. Taliani, M. Sokolowski, E. Umbach, D. Beljonne, J. Cornil, and J. L. Bredás, Phys. Rev. B **62**, 6296 (2000).
[12] P. Petelenz and M. Andrzejak, Chem. Phys. Lett. **343**, 139 (2001).
[13] M. Andrzejak, P. Petelenz, and M. Slawik, J. Chem. Phys. **117**, 1328 (2002).
[14] G. Weiser and S. Möller, Phys. Rev. B **65**, 045203 (2002).
[15] S. Möller, G. Weiser, and C. Taliani, Chem. Phys. **295**, 11 (2003).
[16] H. J. Egelhaaf, J. Giershner, J. Haiber, and D. Oelkrug, Opt. Mater. (Amsterdam, Neth.) **12**, 395 (1999).
[17] D. Oelkrug, H. J. Egelhaaf, and J. Haiber, Thin Solid Films **284-285**, 267 (1996).
[18] W. Gebauer, M. Bassler, R. Fink, M. Sokolowski, and E. Umbach, Chem. Phys. Lett. **266**, 177 (1997).
[19] S. Tavazzi, A. Borghesi, M. Campione, M. Laicini, S. Trabattoni, and P. Spearman, J. Chem. Phys. **120**, 7136 (2004).
[20] M. A. Loi, C. Martin, H. R. Chandrasekhar, M. Chandrasekhar, W. Grauper, F. Garnier, A. Mura, and G. Bongiovanni, Phys. Rev. B **66**, 113102 (2002).
[21] F. Kouki, P. Spearman, P. Valat, G. Horowitz, and F. Garnier, J. Chem. Phys. **113**, 385 (2000).
[22] M. Muccini, E. Lunedei, A. Bree, G. Horowitz, F. Garnier, and C. Taliani, J. Chem. Phys. **108**, 7327 (2000).
[23] T. Siegrist, C. Kloc, R. A. Laudise, H. E. Katz, and R. C. Haddon, Adv. Mater. (Weinheim, Ger.) **10**, 379 (1998).
[24] The correction for the retardation effect evaluated using Ref. 5 is of the order of meV.
[25] V. M. Agranovich and V. L. Ginzburg, *Crystal Optics with Spatial Dispersion and Excitons* (Springer-Verlag, Berlin, 1984).
[26] R. Scholz, A. Y. Kobiski, T. U. Kampen, M. Schreiber, and D. R. T. Zahn, Phys. Rev. B **61**, 13659 (2000).
[27] I. Vragovic, R. Scholz, and M. Schreiber, Europhys. Lett. **57**, 288 (2002).
[28] D. P. Craig and S. H. Walmsley, *Excitons in Molecular Crystals* (W. A. Benjamin, Inc., New York, 1968).
[29] Optimization of planar structure by B3LYP density-functional theory by using 6-31G(d) as basis set with GAUSSIAN98 software.
[30] M. Born and K. Huang, *Dynamical Theory of Crystal Lattices* (Clarendon Press, Oxford, 1968).
[31] L. D. Landau and E. M. Lifshitz, *Electrodynamics of Continous Media* (Pergamon, Oxford, 1977).
[32] D. Birnbaum, D. Fichou, and E. Kohler, J. Chem. Phys. **96**, 165 (1992).
[33] R. S. Becker, J. S. de Melo, A. L. Macanita, and F. Elisei, J. Phys. Chem. **100**, 18 683 (1996).
[34] R. Colditz, D. Grebner, M. Helbig, and S. Rentsch, Chem. Phys. **201**, 309 (1995).
[35] G. Horowitz, S. Romdhane, H. Bouchriha, P. Delannoy, J. Monge, F. Kouki, and P. Valat, Synth. Met. **90**, 187 (1997).
[36] P. Lang, F. Kouki, J. Roger, J. Martinez, G. Horowitz, and F. Garnier, Synth. Met. **101**, 536 (1999).
[37] J. Vrijmoeth, R. W. Stok, R. Veldman, W. A. Schoonveld, and T. M. Klapwijk, J. Appl. Phys. **83**, 3816 (1998).
[38] R. W. Munn, M. Andrzejak, P. Petelenz, A. D. Esposti, and C. Taliani, Chem. Phys. Lett. **336**, 357 (2001).
[39] M. Andrzejak and P. Petelenz, Synth. Met. **109**, 97 (2000).
[40] For the 6-*T* crystal the static dielectric tensor is $\epsilon_{a^*}=6.22$ (calculated in Ref. 38), $\epsilon_b=2.74$ (measured in Ref. 35), $\epsilon_c=3.49$ (measured in Ref. 35). Unfortunately, for the 4-*T* crystal there is no value for the components along the normal to the accessible *ab* surface. Thus we deduced it following the discussions in Ref. 39 and by keeping the same proportionality among the components, we extract the value we used for $\epsilon_{zz}=5.49$, the other two being taken from Refs. 36 and 37.
[41] M. Orrit and P. Kottis, Adv. Chem. Phys. **74**, 1 (1988).
[42] P. Spearman, F. Kouki, P. Lang, P. Valat, G. Horowitz, and F. Garnier, Synth. Met. **119**, 589 (2001).
[43] E. Tosatti and G. Harbeke, Nuovo Cimento Soc. Ital. Fis., B **22**, 87 (1974).
[44] P. Spearman, A. Borghesi, M. Campione, M. Laicini, M. Moret, and S. Tavazzi, J. Chem. Phys. **122**, 014706 (2005).
[45] D. W. Berreman, J. Opt. Soc. Am. **62**, 502 (1972).
[46] M. Schubert, Phys. Rev. B **53**, 4265 (1996).